ACS APPLIED MATERIALS & INTERFACES

Letter

www.acsami.org

Cryogenic Electron Beam Induced Chemical Etching

Aiden A. Martin and Milos Toth*

School of Physics and Advanced Materials, University of Technology, Sydney, 15 Broadway, Ultimo, New South Wales 2007, Australia

Supporting Information

ABSTRACT: Cryogenic cooling is used to enable efficient, gas-mediated electron beam induced etching (EBIE) in cases where the etch rate is negligible at room and elevated substrate temperatures. The process is demonstrated using nitrogen trifluoride (NF_3) as the etch precursor, and Si, SiO_2, SiC, and Si_3N_4 as the materials volatilized by an electron beam. Cryogenic cooling broadens the range of precursors that can be used for EBIE, and enables high-resolution, deterministic etching of materials that are volatilized spontaneously by conventional etch precursors as demonstrated here by NF_3 and XeF_2 EBIE of silicon.

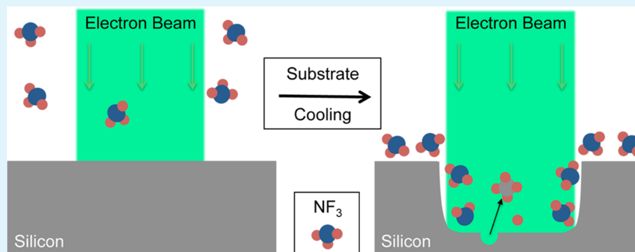

KEYWORDS: *electron beam induced etching, nanofabrication, silicon, nitrogen trifluoride, reaction kinetics, surface chemistry*

Gas-mediated electron beam induced etching (EBIE) enables maskless, beam-directed editing of materials at the nanoscale. Etching has been demonstrated using precursors such as H_2O, O_2, H_2, Cl_2, SF_6, XeF_2, and ClF_3.[1−4] However, the range of precursor−substrate combinations that is appropriate for EBIE has, to date, been small compared to conventional plasma etching[5,6] because many of the precursors that yield radicals responsible for plasma etching have properties that are undesirable for EBIE. Ideally, a substrate etched by EBIE is exposed to a vapor-phase precursor that adsorbs to, but does not etch the material spontaneously. An electron beam is then used to dissociate surface-adsorbed precursor molecules, generating fragments that react with the substrate to produce species that desorb, thereby volatilizing substrate regions near the beam[1] (see inset of Figure 1a). EBIE is typically performed at room temperature because both heating and cooling can inhibit etching by increasing and decreasing the thermal desorption rate of surface-adsorbed precursor molecules and the final reaction products, respectively.

The limited scope of room temperature EBIE is exemplified by nitrogen trifluoride (NF_3), a common fluorine precursor used in laser[7] and plasma[8] induced etching of Si and SiC.[9] NF_3 satisfies most key requirements for EBIE: it has a large electron dissociation cross-section;[10] high vapor pressure; relatively low toxicity and broad material compatibility (in particular, NF_3 does not cause corrosion of components in electron microscope chambers, and does not etch most solids spontaneously, including silicon[11]). Despite these favorable characteristics, NF_3-mediated EBIE has previously not been demonstrated, likely due to poor surface coverage at room temperature. Weak physisorption has been observed on platinum,[12] gold (desorption energy = 0.219 eV)[13] and ruthenium.[14] Standard theory of gas-mediated electron beam processing[1,2,15−22] predicts that the low NF_3 adsorption energies (on the order of 200 meV) give rise to very low etch rates at and near room temperature (see the Supporting Information, section S3). Coverage can, in principle, be increased by substrate cooling since the desorption rate decreases exponentially with reciprocal temperature (see the Supporting Information, section S3). Cooling, however, also inhibits thermal desorption of the final reaction products, and has therefore not been used to enhance EBIE.

Here we show that cryogenic substrate cooling can enable efficient EBIE in cases where the room temperature etch rate is negligible. We demonstrate efficient EBIE of materials that contain Si, C, N and O at temperatures as low as 100 K. The results show that a range of EBIE reaction products can desorb (during electron irradiation) at cryogenic substrate temperatures, and that cryogenic substrate cooling broadens the range of precursors that can be used to realize EBIE. NF_3-mediated EBIE of Si is particularly significant because silicon is most often etched using XeF_2, which gives rise to spontaneous etching and roughening of Si, whereas the electron beam merely accelerates the local etch rate.[23] The only alternatives for EBIE of Si reported to date are SF_6,[24] which is highly inefficient, and Cl_2,[25,26] which is highly corrosive, toxic, and flammable. Cryogenic, NF_3-mediated EBIE overcomes these problems, and enables deterministic, high-resolution editing of Si and associated devices.

EBIE was carried out using an FEI Nova NanoSEM variable pressure[27,28] scanning electron microscope (SEM) equipped with a magnetic immersion lens gaseous secondary electron detector[29] and a liquid nitrogen cooling stage. Substrates used for EBIE were Si, SiO_2, SiC and Si_3N_4. Cylindrical etch pits

Received: September 9, 2014
Accepted: October 21, 2014
Published: October 21, 2014

 © 2014 American Chemical Society

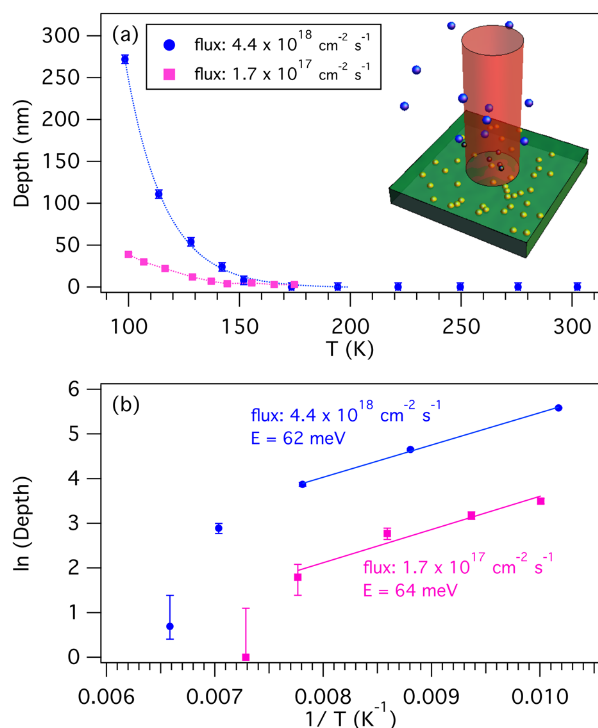

Figure 1. (a) Etch pit depth versus substrate temperature (T) for NF_3-mediated EBIE of Si. (b) Plots used to extract the activation energies E by Arrhenius analyses of the data in (a). Inset: Schematic illustration of electron beam induced etching performed using a stationary beam defocused to attain a top-hat electron flux profile.

were fabricated under 8.4 Pa (8.4×10^{-2} mBar) of NF_3 a using a stationary, 10 keV, 3.4 nA electron beam that under-focused to generate a top-hat flux profile (see the Supporting Information, sections S1a, b, for additional details). This configuration, shown schematically in the inset of Figure 1, yields conditions that are optimal for quantitative analysis of EBIE rates.[3,20,22,30] The temperature was always above the condensation point of the precursor gas (see the Supporting Information, section S1c), in contrast to ice lithography and cryogenic electron beam induced deposition.[31−34]

Comparisons to Cl_2-mediated EBIE of Si (Figure 3a) were performed using the electron exposure conditions used by Roediger et al.,[25,26] an NF_3 pressure of 6.5 Pa and a substrate temperature of 106 K. Delocalized etching of Si caused by XeF2 precursor vapor (Sigma-Aldrich, 99.99%) was demonstrated (Figure 3b) using a gas injection capillary located ∼100 μm from the substrate surface in high vacuum (∼3.8×10^{-3} Pa), at room temperature (see the Supporting Information, section S1d). A framed "NF_3" symbol (Figure 4) was etched into Si by a 20 keV, 9.9 nA electron beam, using an NF_3 pressure of 6.5 Pa and a substrate temperature of 106 K. Total processing time was 5 min with an electron beam dwell time of 13 ms per pixel.

Figures 1a, b show plots of the depth of pits made in Si (measured using an atomic force microscope (AFM), see the Supporting Information section S1f) by NF_3-mediated EBIE as a function of temperature (T). The etch rate is negligible at room temperature and increases as the substrate temperature is reduced to ∼98 K. At any given temperature, the etch rate is constant with time (over the experimental time scale), as seen in Figure 2.

Figure 1b shows that the etch rate scales exponentially with $1/T$ at reciprocal temperatures greater than ∼0.0075 K^{-1}. At

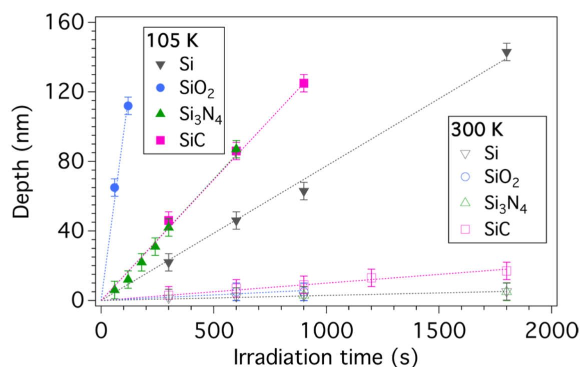

Figure 2. Etch pit depth versus time measured for Si, SiO_2, SiC, and Si_3N_4 etched by NF_3-mediated EBIE at substrate temperatures of 105 and 300 K.

lower values of $1/T$ (i.e., higher temperatures), EBIE is inhibited through a thermally activated mechanism that we ascribe tentatively to surface diffusion of residual contaminants (such as hydrocarbons and H_2O)[35,36] present at the substrate surface. Residual contaminants compete for surface sites with NF_3 adsorbates and can therefore inhibit EBIE, particularly at elevated temperatures where the NF_3 coverage is low and diffusivity (of all species at the surface) is relatively high.

At reciprocal temperatures greater than ∼0.0075 K^{-1}, the exponential increase in etch rate with $1/T$ is attributed to a corresponding increase in the surface coverage of NF_3 caused by a decrease in the NF_3 residence time at the substrate surface (see the Supporting Information, section S3). We note that an exponential increase in EBIE rate with $1/T$ can not be explained by the temperature-dependence of the adsorbate diffusion coefficient which decreases with $1/T$ (see the Supporting Information, section S3).

In our experiments, analysis of the EBIE reaction products by mass spectrometry was not possible due to the high NF_3 pressure and small quantity of volatile molecules generated in EBIE. However, based on other dry chemical etch processes,[37] and XeF_2-mediated EBIE of Si,[38] the etch reaction products are most likely of the form SiF_n, where n = 1−4, and the thermal desorption rate increases as $n \to 4$.[39]

The etch pit depth data shown in Figure 1b can be used to extract the thermal activation energy (E) of the process responsible for the observed temperature dependence. Arrhenius analyses of the curves yield an activation energy of ∼63 ± 1 meV for EBIE performed using electron fluxes of 1.7×10^{17} cm^{-2} s^{-1} and 4.4×10^{18} cm^{-2} s^{-1}, respectively. This value of E serves as a lower limit for the adsorption energy of NF_3, as discussed in the Supporting Information (sections S4 and S5).

NF_3-mediated EBIE was also applied to silicon oxide, carbide and nitride to determine the etch efficiency of materials other than Si. The etch rates of all three compounds are very low at room temperature, and increase significantly at the cryogenic temperature of 105 K, as seen in Figure 2. The volumetric etch rates at cryogenic temperature are 9.1×10^4, 1.1×10^6, 1.6×10^5, and 1.6×10^5 nm^3 s^{-1} for Si, SiO_2, Si_3N_4, and SiC, respectively. SiO_2 exhibited the highest volumetric etch rate, likely because of the existence of additional reaction pathways enabled by oxygen, such as the generation of $SiOF_2$[40] and OF species,[41] and a lower concentration of silicon atoms in the material.

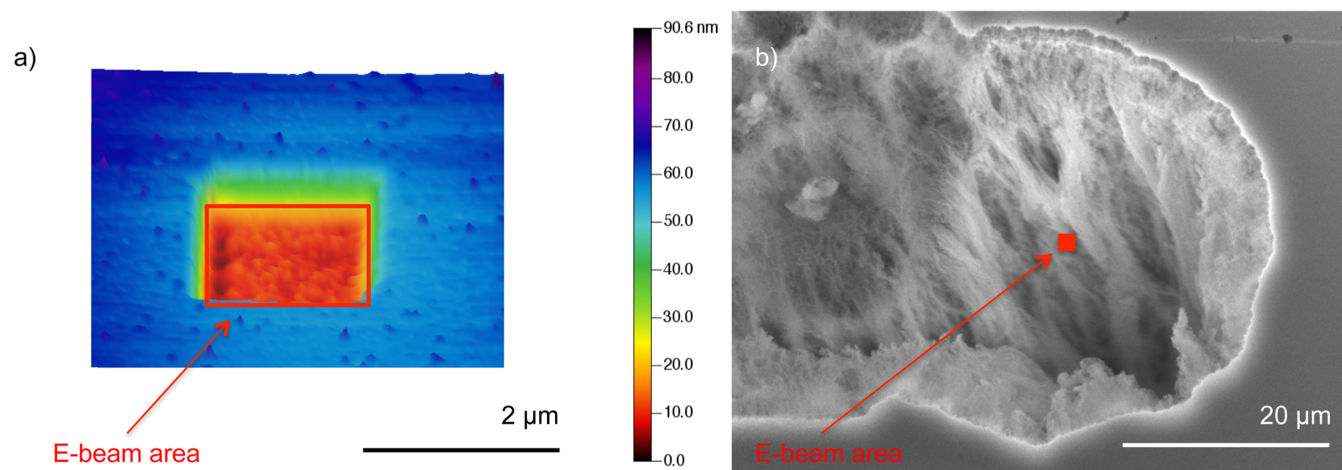

Figure 3. (a) AFM image of a rectangular pit made in Si by NF_3-mediated EBIE, illustrating the absence of delocalized damage produced by spontaneous etching of Si. (b) SEM image of Si processed by XeF_2-mediated EBIE using the same electron exposure parameters as those used in (a). Red rectangles show the areas that were scanned by the electron beam and correspond to the nominal areas of etch pits made by EBIE. The image in (b) shows delocalized damage caused by spontaneous etching of Si by XeF_2 that occurred during EBIE.

In the case of SiO_2 and Si_3N_4, the desorption of nitrogen and oxygen is not surprising at cryogenic temperatures. However, the carbon present in SiC needs to be volatilized by radicals produced by electron dissociation of NF_3 adsorbates. The volatile reaction products are most likely of the form CF_x (where $x = 1-4$).

Next, we compare the efficacy of the cryogenic NF_3 etch process to room temperature alternatives reported to date in the EBIE literature. Electron exposure conditions used by Roediger et al. for Cl_2-mediated EBIE of Si[25,26] were replicated using XeF_2 and NF_3. The use of XeF_2 results in highly delocalized damage, caused by rapid spontaneous etching of Si. For example, Figure 3b shows a substrate region that contains an etch box with a nominal area of 1.5×1.5 μm, and a region of severe damage produced by XeF_2 that extends ~20 μm from the rectangle scanned by the beam. Such rapid, delocalized etching by XeF_2 is typical when the native oxide layer is compromised (by pinhole defects, or by EBIE). This behavior is clearly unfavorable as it inhibits the ability to etch Si with high spatial resolution (see the Supporting Information, section S1e). In comparison, NF_3-mediated EBIE did not give rise to any observable spontaneous etching of the Si substrate. Instead, it yielded a well-defined etch pit with a depth of ~55 nm (Figure 3a), and a volumetric etch rate that is ~2.4 times greater than that of Cl_2 under the same electron exposure conditions.

A complex pattern etched into Si using NF_3 is shown in Figure 4. It demonstrates high-resolution, localized editing of Si in the absence of highly toxic, flammable and corrosive precursors that are unsuitable for use in electron microscopes (ultimate EBIE resolution is governed by the electron beam diameter, proximity effects and material roughening that occurs during etching).[42] We note that SF_6 has also been reported as a precursor for room-temperature EBIE of Si.[24] This etch process is, however, extremely inefficient and inappropriate for high-resolution EBIE, and may give rise to unintended deposition of sulfur.[43]

In summary, cryogenic cooling was used to enable efficient gas-mediated electron beam induced etching using nitrogen trifluoride as the etch precursor. The etch rate is limited by thermal desorption of weakly bound NF_3 adsorbates. The process was demonstrated using Si, SiO_2, SiC, and Si_3N_4, and enables high-resolution EBIE in the absence of artifacts caused by delocalized spontaneous etching of the substrates.

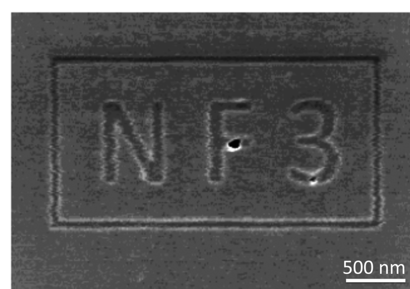

Figure 4. SEM image of a framed "NF_3" symbol etched into Si by NF_3-mediated EBIE with a line resolution of ~85 nm.

ASSOCIATED CONTENT

Supporting Information

S1, notes; S2, modeling introduction; S3, temperature dependence of electron beam induced etching; S4, Arrhenius analysis of single step EBIE reactions; S5, Arrhenius analysis of multistep EBIE reactions; S6, model input parameters. This material is available free of charge via the Internet at http://pubs.acs.org.

AUTHOR INFORMATION

Corresponding Author

*E-mail: Milos.Toth@uts.edu.au.

Notes

The authors declare no competing financial interest.

ACKNOWLEDGMENTS

This work was funded by FEI Company. A.M. is the recipient of a John Stocker Postgraduate Scholarship from the Science and Industry Endowment Fund.

REFERENCES

(1) Utke, I.; Moshkalev, S.; Russell, P. *Nanofabrication Using Focused Ion and Electron Beams: Principles and Applications*; Oxford University Press: New York, 2012.

(2) Randolph, S. J.; Fowlkes, J. D.; Rack, P. D. Focused, Nanoscale Electron-Bearn-Induced Deposition and Etching. *Crit. Rev. Solid State Mater. Sci.* **2006**, *31*, 55−89.
(3) Toth, M. Advances in Gas-Mediated Electron Beam-Induced Etching and Related Material Processing Techniques. *Appl. Phys. A: Mater. Sci. Process.* **2014**, DOI: 10.1007/s00339-014-8596-8.
(4) Rack, P.; Randolph, S.; Deng, Y.; Fowlkes, J.; Choi, Y.; Joy, D. C. Nanoscale Electron-Beam-Stimulated Processing. *Appl. Phys. Lett.* **2003**, *82*, 2326−2328.
(5) Winters, H. F.; Coburn, J. W. Surface Science Aspects of Etching Reactions. *Surf. Sci. Rep.* **1992**, *14*, 161−269.
(6) Flamm, D. L. Mechanisms of Silicon Etching in Fluorine-and Chlorine-Containing Plasmas. *Pure Appl. Chem.* **1990**, *62*, 1709−1720.
(7) Brannon, J. H. Chemical Etching of Silicon by CO_2 Laser-Induced Dissociation of NF_3. *J. Vac. Sci. Technol., B* **1987**, *5*, 1399−1399.
(8) Bruno, G.; Capezzuto, P.; Cicala, G.; Manodoro, P. Study of the NF_3 Plasma Cleaning of Reactors for Amorphous Silicon Deposition. *J. Vac. Sci. Technol., A* **1994**, *12*, 690−698.
(9) Tasaka, A.; Takahashi, K.; Tanaka, K.; Shimizu, K.; Mori, K.; Tada, S.; Shimizu, W.; Abe, T.; Inaba, M.; Ogumi, Z.; Tojo, T. Plasma Etching of SiC Surface Using NF_3. *J. Vac. Sci. Technol., A* **2002**, *20*, 1254−1260.
(10) Haaland, P. D.; Jiao, C. Q.; Garscadden, A. Ionization of NF_3 by Electron Impact. *Chem. Phys. Lett.* **2001**, *340*, 479−483.
(11) Miotto, R.; Ferraz, A.; Srivastava, G. Dissociative Adsorption of NF_3 on Si(001)-(2 × 1). *Surf. Sci.* **2000**, *454−456*, 152−156.
(12) Junker, K. H.; White, J. Adsorption of NF_3 on Pt(111): Interactions with Electrons and Photons. *Surf. Sci.* **1997**, *382*, 67−78.
(13) Rzeźnicka, I. I.; Lee, J.; Yates, J. T., Jr. Dynamics of NF_3 in a Condensed Film on Au(111) as Studied by Electron-Stimulated Desorption. *Surf. Sci.* **2006**, *600*, 4492−4500.
(14) Walczak, M.; Johnson, A.; Thiel, P.; Madey, T. The Interaction of NF_3 with Ru (0001): Order at Steps. *J. Vac. Sci. Technol., A* **1988**, *6*, 675−680.
(15) Utke, I.; Hoffmann, P.; Melngailis, J. Gas-Assisted Focused Electron Beam and Ion Beam Processing and Fabrication. *J. Vac. Sci. Technol., B* **2008**, *26*, 1197−1276.
(16) Huth, M.; Porrati, F.; Schwalb, C.; Winhold, M.; Sachser, R.; Dukic, M.; Adams, J.; Fantner, G. Focused Electron Beam Induced Deposition: A Perspective. *Beilstein J. Nanotechnol.* **2012**, *3*, 597−619.
(17) Lassiter, M. G.; Rack, P. D. Nanoscale Electron Beam Induced Etching: A Continuum Model that Correlates the Etch Profile to the Experimental Parameters. *Nanotechnology* **2008**, *19*, 455306.
(18) Smith, D. A.; Fowlkes, J. D.; Rack, P. D. Understanding the Kinetics and Nanoscale Morphology of Electron-Beam-Induced Deposition Via a Three-Dimensional Monte Carlo Simulation: The Effects of the Precursor Molecule and the Deposited Material. *Small* **2008**, *4*, 1382−1389.
(19) Fowlkes, J. D.; Rack, P. D. Fundamental Electron-Precursor-Solid Interactions Derived from Time-Dependent Electron-Beam-Induced Deposition Simulations and Experiments. *ACS Nano* **2010**, *4*, 1619−1629.
(20) Randolph, S.; Toth, M.; Cullen, J.; Chandler, C.; Lobo, C. Kinetics of Gas Mediated Electron Beam Induced Etching. *Appl. Phys. Lett.* **2011**, *99*, 213103.
(21) Bishop, J.; Lobo, C. J.; Martin, A.; Ford, M.; Phillips, M. R.; Toth, M. The Role of Activated Chemisorption in Electron Beam Induced Deposition. *Phys. Rev. Lett.* **2012**, *109*, 146103.
(22) Martin, A.; Phillips, M. R.; Toth, M. Dynamic Surface Site Activation: A Rate Limiting Process in Electron Beam Induced Etching. *ACS Appl. Mater. Interfaces* **2013**, *5*, 8002−8007.
(23) Matsui, S.; Mori, K. Direct Writing onto Si by Electron Beam Stimulated Etching. *Appl. Phys. Lett.* **1987**, *51*, 1498−1499.
(24) Vanhove, N.; Lievens, P.; Vandervorst, W. Electron Beam Induced Etching of Silicon with SF_6. *J. Vac. Sci. Technol., B* **2010**, *28*, 1206−1209.
(25) Roediger, P.; Wanzenboeck, H.; Hochleitner, G.; Bertagnolli, E.; Buehler, W. Focused Electron Beam Induced Etching of Silicon by Chlorine Gas: Negative Effects of Residual Gas Contamination on the Etching Process. *J. Appl. Phys.* **2010**, *108*, 124316.
(26) Roediger, P.; Hochleitner, G.; Bertagnolli, E.; Wanzenboeck, H.; Buehler, W. Focused Electron Beam Induced Etching of Silicon Using Chlorine. *Nanotechnology* **2010**, *21*, 285306.
(27) Danilatos, G. D. Foundations of Environmental Scanning Electron Microscopy. *Adv. Electron. Electron Phys.* **1988**, *71*, 109−250.
(28) Thiel, B. L.; Toth, M. Secondary Electron Contrast in Low-Vacuum/Environmental Scanning Electron Microscopy of Dielectrics. *J. Appl. Phys.* **2005**, *97*, 051101.
(29) Thiel, B.; Toth, M.; Schroemges, R. P. M.; Scholtz, J. J.; van Veen, G.; Knowles, W. Two-Stage Gas Amplifier for Ultrahigh Resolution Low Vacuum Scanning Electron Microscopy. *Rev. Sci. Instrum.* **2006**, *77*, 033705−7.
(30) Lobo, C. J.; Martin, A.; Phillips, M. R.; Toth, M. Electron Beam Induced Chemical Dry Etching and Imaging in Gaseous NH_3 Environments. *Nanotechnology* **2012**, *23*, 375302.
(31) Bresin, M.; Thiel, B. L.; Toth, M.; Dunn, K. A. Focused Electron Beam-Induced Deposition at Cryogenic Temperatures. *J. Mater. Res.* **2011**, *26*, 357−364.
(32) Bresin, M.; Toth, M.; Dunn, K. A. Direct-Write 3D Nanolithography at Cryogenic Temperatures. *Nanotechnology* **2013**, *24*, 035301.
(33) King, G. M.; Schürmann, G.; Branton, D.; Golovchenko, J. A. Nanometer Patterning with Ice. *Nano Lett.* **2005**, *5*, 1157−1160.
(34) Gardener, J. A.; Golovchenko, J. A. Ice-Assisted Electron Beam Lithography of Graphene. *Nanotechnology* **2012**, *23*, 185302.
(35) Perentes, A.; Hoffmann, P. Oxygen Assisted Focused Electron Beam Induced Deposition of Si-Containing Materials: Growth Dynamics. *J. Vac. Sci. Technol., B* **2007**, *25*, 2233−2238.
(36) Li, J.; Toth, M.; Tileli, V.; Dunn, K. A.; Lobo, C. J.; Thiel, B. L. Evolution of the Nanostructure of Deposits Grown by Electron Beam Induced Deposition. *Appl. Phys. Lett.* **2008**, *93*, 023130.
(37) Jansen, H.; Gardeniers, H.; Boer, M. d.; Elwenspoek, M.; Fluitman, J. A Survey on the Reactive Ion Etching of Silicon in Microtechnology. *J. Micromech. Microeng.* **1999**, *6*, 14−28.
(38) Vanhove, N.; Lievens, P.; Vandervorst, W. Particle Emission from Chemically Enhanced Electron-Beam-Induced Etching of Si: An Approach for Zero-Energy Secondary-Ion Mass Spectrometry. *Phys. Rev. B: Condens. Matter Mater. Phys.* **2009**, *79*, 035305.
(39) Vugts, M. J. M. Si/XeF_2 Etching: Temperature Dependence. *J. Vac. Sci. Technol., A* **1996**, *14*, 2766−2774.
(40) Hills, M. M. The Interaction of XeF_2 with Sapphire. *Appl. Surf. Sci.* **1994**, *78*, 165−177.
(41) Kastenmeier, B. E. E.; Matsuo, P. J.; Oehrlein, G. S.; Langan, J. G. Remote Plasma Etching of Silicon Nitride and Silicon Dioxide Using NF_3/O_2 Gas Mixtures. *J. Vac. Sci. Technol., A* **1998**, *16*, 2047−2056.
(42) Toth, M.; Lobo, C.; Knowles, W.; Phillips, M.; Postek, M.; Vladár, A. Nanostructure Fabrication by Ultra-High-Resolution Environmental Scanning Electron Microscopy. *Nano Lett.* **2007**, *7*, 525−530.
(43) Mattausch, H. J. Reactive Ion Etching of Ta-Silicide/Polysilicon Double Layers for the Fabrication of Integrated Circuits. *J. Vac. Sci. Technol., B* **1983**, *1*, 15−22.